

## Small Ion-Temperature-Gradient Scale Length and Reduced Heat Diffusivity at Large Hydrogen Isotope Mass in Conventional $H$ -Mode Plasmas

H. Urano,<sup>1</sup> T. Takizuka,<sup>2</sup> M. Kikuchi,<sup>1</sup> T. Nakano,<sup>1</sup> N. Hayashi,<sup>1</sup> N. Oyama,<sup>1</sup> and Y. Kamada<sup>1</sup>

<sup>1</sup>Japan Atomic Energy Agency, Naka Fusion Institute, Naka, Ibaraki 311-0193, Japan

<sup>2</sup>Osaka University, Suita, Osaka 565-0871, Japan

(Received 19 May 2012; published 18 September 2012; publisher error corrected 20 September 2012)

The dependence of the ion-temperature-gradient scale length on the hydrogen isotope mass was examined in conventional  $H$ -mode plasmas in JT-60U tokamak. While identical profiles for density and temperature were obtained for hydrogen and deuterium plasmas, the ion conductive heat flux necessary for hydrogen to sustain the same ion temperature profile was two times that required for deuterium, resulting in a clearly higher ion heat diffusivity for hydrogen at the same ion-temperature-gradient scale length. On the other hand, the ion-temperature-gradient scale length for deuterium is less than that for hydrogen at a given ion heat diffusivity.

DOI: 10.1103/PhysRevLett.109.125001

PACS numbers: 52.25.Fi, 52.35.Ra, 52.55.Fa

Knowledge of the influence of the hydrogen isotope composition on heat conduction in fusion plasmas is essential for accurately projecting the energy confinement times in future burning plasma devices that will use a mixture of deuterium and tritium. Reduced energy confinement at lighter hydrogen isotopes has been empirically observed for  $H$ -mode plasmas in many devices [1–4]. For all these observations, the energy confinement time increased with the isotope mass ratio in the form  $\tau_{\text{th}} \propto M^\zeta$  with the exponent  $\zeta$  greater than 0. While the favorable dependence of the energy confinement on the isotope mass has led to optimistic visions for a future reactor, the underlying physics behind the role of the hydrogen isotope composition has not been understood for the last three decades.

$H$ -mode plasma is characterized by an edge pedestal component which is determined by the magnetohydrodynamic destabilization of edge-localized-modes and a core component which is governed by the turbulent transport that originates in the microinstabilities. In present understanding, particularly of the core plasma, it is believed that turbulence driven by ion-temperature-gradient (ITG) is the main cause for the anomalous heat transport through the ion channel in tokamaks [5,6]. The ion temperature profiles are limited by a strong increase in the transport when the temperature gradient scale length  $L_{T_i} (= T_i / \nabla T_i)$  exceeds the critical value  $L_{T_i}^c$ . Under this situation, the ion heat diffusivity  $\chi_i$  can be described by:

$$\chi_i = \chi_{i0} + \xi_{\text{ITG}} f(R/L_{T_i} - R/L_{T_i}^c), \quad (1)$$

where  $\chi_{i0}$  represents the ion heat diffusivity in the absence of TG turbulence, which consists mainly of neoclassical transport, and  $R$  is the major radius. The product  $\xi_{\text{ITG}} f$  represents the ion heat diffusivity caused by the ITG turbulence. The function  $f$  is equal to zero for  $L_{T_i} \geq L_{T_i}^c$  but increases rapidly when  $L_{T_i} < L_{T_i}^c$ . When  $L_{T_i} < L_{T_i}^c$ ,

transport is enhanced to keep  $L_{T_i}$  close to  $L_{T_i}^c$  providing the stiff temperature profile.

Experimental observations of the strong correlation between the edge and core  $T_i$  values serve as qualitatively supportive evidence of this theoretical picture [7–10]. For the interest of predicting the energy confinement that would lead to possible fusion power in a reactor, the experimental characterization of heat transport has been well developed. However, little is known about the processes responsible for heat transport by varying the hydrogen isotope composition. The modeling of such anomalous transport processes for  $H$ -mode plasmas strongly requires the experimental evidence obtained from a set of different isotope species. The study on the isotope effect on the energy confinement was originally motivated by the fact that the enhancement of the ion heat transport which depends on the ion Larmor radius  $\rho_i$  ( $\propto M^{1/2}$ ) in most theoretical models, such as gyro-Bohm diffusion, apparently contradicts the observation of the enhanced confinement obtained with heavy hydrogen isotopes.

This Letter presents the dependence of ion heat transport on the hydrogen isotope mass in conventional  $H$ -mode plasmas from the view point of the TG scale length of the ion temperature profiles at the plasma core. To accomplish this goal, a series of experiments on hydrogen and deuterium  $H$ -mode plasmas using variable heating power with a neutral beam (NB) was analyzed in JT-60U tokamak. The experiments were conducted at a plasma current  $I_p = 1.08$  MA and a toroidal magnetic field  $B_t = 2.4$  T at a given magnetic geometry with a major radius  $R = 3.36$  m and a minor radius  $a = 0.86$  m [11]. The remaining geometrical parameters were also fixed with an ellipticity  $\kappa = 1.4$ , a triangularity  $\delta = 0.36$ , and a safety factor at 95% flux surface  $q_{95} = 3.7$ . The line-averaged electron density remained nearly constant at  $\bar{n}_e = 2.3\text{--}2.5 \times 10^{19} \text{ m}^{-3}$ . A positive-ion-based NB (PNB) with an accelerating energy  $E_b$  of  $\sim 85$  keV was applied in the

$P_{\text{NBI}}$  range of 5–15 MW, which was sufficient to examine the ITG scale length relative to the local ion heat flux.

Figure 1 shows the thermal energy confinement time  $\tau_{\text{th}}$  as a function of the loss power  $P_L$  in this series of experiments. The  $\tau_{\text{th}}$  value decreases continuously with  $P_L$  for both hydrogen and deuterium at approximately the same scale, as expected from the empirical law  $\tau_{\text{th}} \propto P_L^{-0.69}$  [12]. However,  $\tau_{\text{th}}$  is larger by approximately a factor of 1.2–1.3 for deuterium in comparison with that for hydrogen at a given  $P_L$ . The effective ion charge number  $Z_{\text{eff}}$  is  $\sim 1.5$  at  $P_L \leq 5$  MW in both cases. The  $Z_{\text{eff}}$  for deuterium increases continuously with the heating power and reaches  $\sim 2.4$  at  $P_L$  of  $\sim 8$  MW, while it remains constant at  $\sim 1.5$  for hydrogen. The gray line in Fig. 1 indicates the constant thermal stored energy  $W_{\text{th}} (= 0.75$  MJ) when a steady state ( $dW/dt \sim 0$ ) is reached. A pair of hydrogen and deuterium plasmas with the same  $W_{\text{th}}$  were chosen along this line for comparison of the heat transport analysis, as indicated by (A) and (B), respectively. The power required to sustain the same  $W_{\text{th}}$  was greater for hydrogen ( $P_L = 8.0$  MW) than for deuterium ( $P_L = 4.0$  MW) by a factor of 2, resulting in the  $\tau_{\text{th}}$  value ( $= W_{\text{th}}/P_L$ ) of 0.1 s for hydrogen, which was half that for deuterium ( $\tau_{\text{th}} = 0.2$  s). The  $Z_{\text{eff}}$  value of  $\sim 1.5$  was nearly the same for both cases. The heat diffusivity is estimated by the 1.5-dimensional (two-dimensional equilibrium and one-dimensional transport) transport analysis code (TOPICS) [13].

The results of the heat transport analyses for these two cases are shown in Fig. 2. In the figure, the spatial profiles of  $T_i$  and  $n_e$  become obviously identical [see Figs. 2(a) and 2(b), respectively]. It is worth noting that the profiles of the electron temperatures  $T_e$  are also very similar, indicating that the spatial profiles of the thermal pressures  $p_{\text{th}}$ , and thus, the  $W_{\text{th}}$  values, also become approximately identical. The ion conductive heat flux  $Q_i$  for hydrogen becomes approximately two times that for

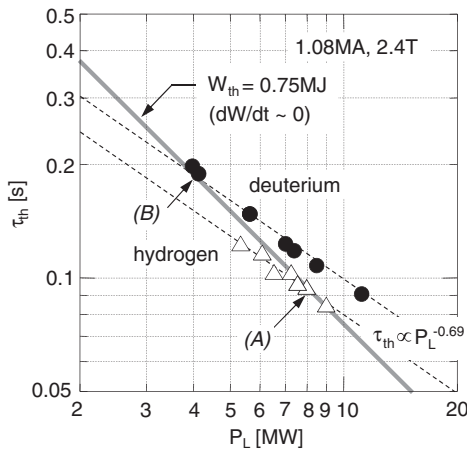


FIG. 1. Dependence of the thermal energy confinement time  $\tau_{\text{th}}$  on the loss power  $P_L$  for deuterium and hydrogen  $H$ -mode plasmas performed at 1.08 MA and 2.4 T. A pair of plasmas with  $W_{\text{th}} (= P_L \tau_{\text{th}})$  of 0.75 MJ are indicated as (A) and (B).

deuterium [see Fig. 2(c)], which corresponds to the result that two times as much heating power is required for hydrogen. Hence, the  $\chi_i$  values for hydrogen are explicitly higher throughout the minor radius compared with those for deuterium as shown in Fig. 2(d). The source heat flux of ions is responsible for nearly 40% of the total source heat flux for both cases. Besides, the  $Q_i$  occupies  $\sim 70\%$  of the ion source heat flux.

Since  $\chi_i$  in the power balance equation is determined by  $Q_i/n_i \nabla T_i$  in the steady state, the ion heat transport can be characterized in a diagram of the ion conductive heat flux divided by the ion density  $Q_i/n_i$  and the ion temperature gradient  $\nabla T_i$ . As shown in Fig. 3, the  $(Q_i/n_i, \nabla T_i)$  diagram is evaluated at  $r/a = 0.6$ , where the influence of the local heat transport on the overall energy confinement becomes significant in standard  $H$ -mode plasmas. In this diagram, the angle  $\theta$  formed between the horizontal axis and a straight line that passes through both the data and the origin of the coordinates corresponds to the ion heat diffusivity  $\chi_i (= \tan \theta)$ . Because the increase in  $\nabla T_i$  is less significant than that in  $Q_i/n_i$ ,  $\chi_i$  increases gradually with the heating power for both hydrogen and deuterium. In further detail, the increase in  $\chi_i$  with the heating power is more rapid for hydrogen than for deuterium, suggesting a reduced energy confinement for hydrogen plasmas. Simultaneously, the increase in  $\nabla T_i$  is less intense for hydrogen than for deuterium. In this experiment, due to lower neutralization efficiency of NBI for hydrogen, which becomes half that for deuterium, a larger number of perpendicular NB units were injected for hydrogen to compensate for a shortage of  $P_{\text{NBI}}$  in comparison with the  $P_{\text{NBI}}$  range for deuterium. This operation leads to a larger ripple loss of fast ions,

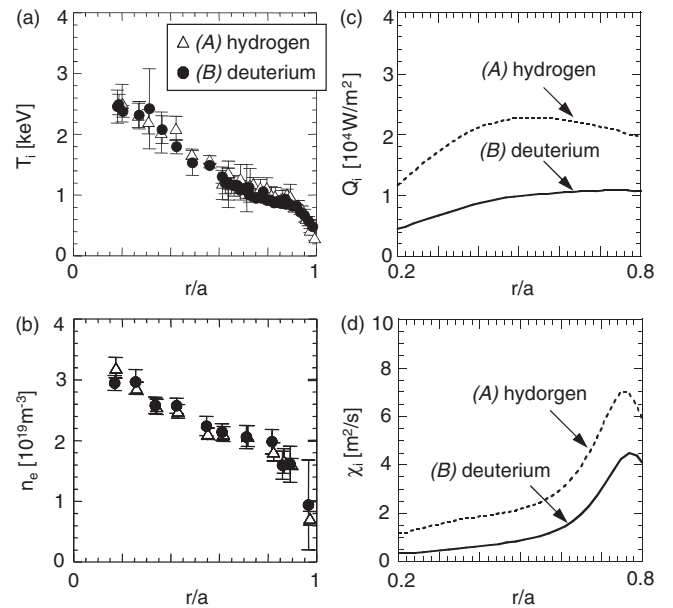


FIG. 2. Profiles of (a)  $T_i$ , (b)  $n_e$ , (c)  $Q_i$ , and (d)  $\chi_i$  for the hydrogen and deuterium plasmas with the same  $W_{\text{th}}$  of 0.75 MJ indicated as (A) and (B) in Fig. 1.

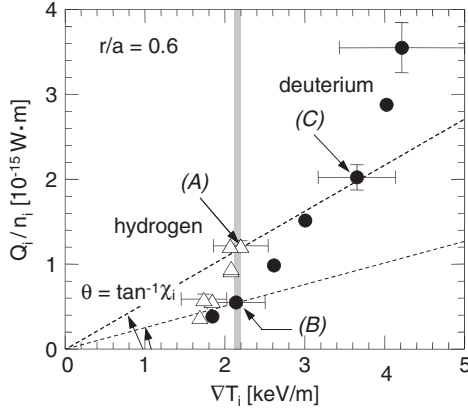


FIG. 3. Relationship between  $Q_i/n_i$  and  $\nabla T_i$  evaluated at  $r/a = 0.6$ . The data for hydrogen and deuterium with the same  $W_{th}$  of 0.75 MJ are indicated as (A) and (B), respectively.

which enhances the toroidal rotation velocity  $V_T$  for hydrogen slightly toward the counter direction by  $\sim 10$  krad/s at  $r/a = 0.6$  on the average. There is a possibility that the  $V_T$  value may change the stability boundary of the pressure gradient at the plasma edge [14,15]. However, the reduction of  $L_{T_i}$  due to  $V_T$  is not clearly present with a similar range of the  $V_T$  variation near  $r/a = 0.6$  in JET tokamak [16] and is not observed in a wide variation of the toroidal momentum input in conventional  $H$ -modes without an internal transport barrier in JT-60U [17]. The difference of  $V_T$  between hydrogen and deuterium is much smaller than the experiment on the  $V_T$  scan.

In Fig. 3, the data points (A) and (B) with the same  $W_{th}$  of 0.75 MJ are plotted along the same  $\nabla T_i$  of  $\approx 2.1$  keV/m at  $r/a = 0.6$  because of the identical  $T_i$  profiles. However, the  $Q_i/n_i$  value increases for hydrogen compared with that for deuterium by a factor of 2, resulting in a  $\chi_i$  value that is two times as large for hydrogen.

Along the straight line passing through the hydrogen data point (A), there is a deuterium data point indicated as (C) in Fig. 3. This pair of hydrogen and deuterium plasmas have similar  $\chi_i$  values of 3.0–3.1  $\text{m}^2/\text{s}$  at  $r/a = 0.6$  while both  $\nabla T_i$  and  $Q_i/n_i$  are higher for deuterium (C) than for hydrogen (A). Figure 4 shows the results of the heat transport analysis for these two cases. The  $T_i$  values increase for deuterium throughout the minor radius to a greater extent in comparison with those for hydrogen while the  $n_e$  profiles are nearly identical [see Figs. 4(a) and 4(b)]. The  $Z_{eff}$  of  $\sim 2.3$  for deuterium is higher than the  $Z_{eff}$  of  $\sim 1.5$  for hydrogen, indicating that the deuterium ion density is lower by  $\sim 20\%$  than the hydrogen ion density on the assumption that carbon is the main impurity content. The  $Q_i$  value for deuterium at  $r/a > 0.4$  increases in comparison with that for hydrogen [see Fig. 4(c)], and the spatial profiles of  $\chi_i$  are nearly identical [see Fig. 4(d)]. Despite having nearly the same profiles of  $Q_i$  and  $\chi_i$  at  $r/a \leq 0.4$ , the higher  $T_i$  for deuterium evidently leads to a contribution from the outside of the flux surface as a boundary

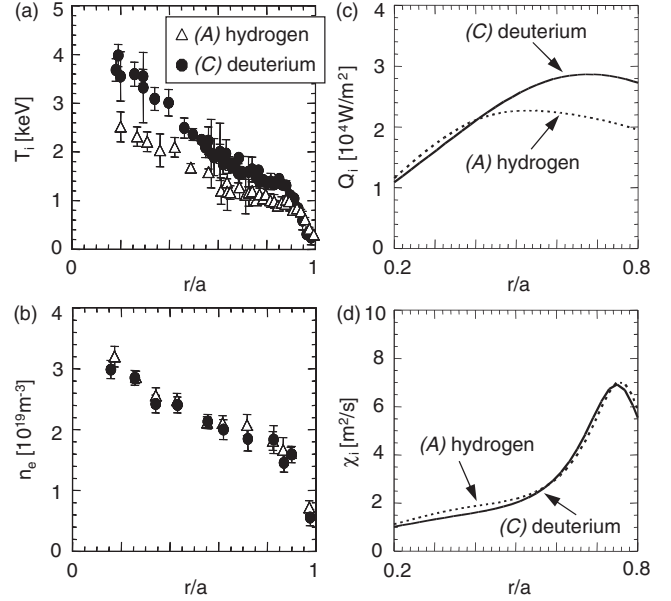


FIG. 4. Profiles of (a)  $T_i$ , (b)  $n_e$ , (c)  $Q_i$ , and (d)  $\chi_i$  for the hydrogen and deuterium plasmas with similar  $\chi_i$  values indicated as (A) and (C) in Fig. 3.

condition for the profile stiffness. Note that the  $P_L$  values for hydrogen (A) and deuterium (C) are 8.0 MW and 7.4 MW, respectively, while the ion conductive heat flux  $Q_i$  of  $2.2 \times 10^4$   $\text{W}/\text{m}^2$  at  $r/a = 0.6$  is smaller for (A) in comparison with  $Q_i$  of  $2.7 \times 10^4$   $\text{W}/\text{m}^2$  for (C). This difference in results occurs because the critical energy  $E_c$  of the NBI, where the power transferred to the ions becomes equivalent to that of the electrons, scales as  $E_c \propto M^{1/3}$ . Under the condition with the accelerating energy  $E_b$  of 85 keV, which is basically below or comparable to the  $E_c$  in standard  $H$ -mode plasmas for both hydrogen and deuterium, the fraction of the ion heating power becomes relatively more dominant for deuterium by a factor of  $2^{1/3}$  in comparison with that for hydrogen at a given  $P_L$ . Accordingly, the resultant  $Q_i$  value is higher as shown in Fig. 4(c).

Figure 5 shows the relationship between  $\chi_i$  and  $\nabla T_i/T_i$  (or  $R/L_{T_i}$ ) at  $r/a = 0.6$ . It can be seen in this figure that  $\chi_i$  increases rapidly with  $\nabla T_i/T_i$  for both the hydrogen and deuterium plasmas, indicating the profile stiffness for the variation of the heating power in this experiment. However, the  $\nabla T_i/T_i$  values required for a given  $\chi_i$  clearly increased by a factor of  $\sim 1.2$  for deuterium in comparison with those for hydrogen, as is shown with the plotted pair of data points (A) and (C), which have similar  $\chi_i$  at different  $\nabla T_i/T_i$ . On the other hand, Fig. 5 also shows the pair of data points (A) and (B) with the same  $W_{th}$ . As expected from the identical  $T_i$  profiles in Fig. 2, the  $\chi_i$  at  $r/a = 0.6$  is two times as large for hydrogen than for deuterium with the same  $\nabla T_i/T_i$  of  $\sim 2.0$   $\text{m}^{-1}$  (or  $R/L_{T_i} \sim 7.0$ ); this result is also indicative of a decrease in the  $L_{T_i}$  value with increasing hydrogen isotope mass.

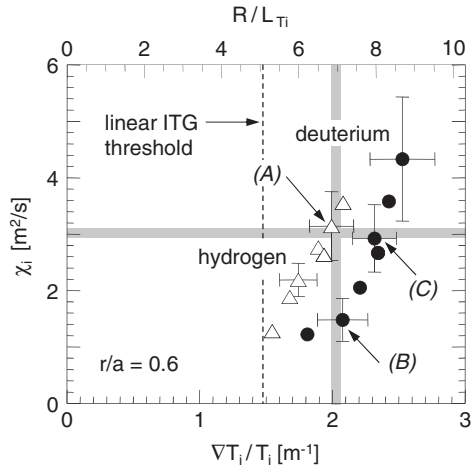


FIG. 5. Ion heat diffusivity  $\chi_i$  as a function of  $\nabla T_i/T_i$  (or  $R/L_{T_i}$ ) at  $r/a = 0.6$  for hydrogen and deuterium  $H$ -mode plasmas.

In discussion, the linear ITG threshold is predicted by an analytical formula [18] expressed as:

$$R/L_{T_i}^c = \frac{4}{3} \left( 1 + \frac{T_i}{T_e} \right) \left( 1 + 2 \frac{s}{q} \right), \quad (2)$$

where  $s$  denotes the magnetic shear. This equation holds under the condition where  $R/L_n < 2(1 + T_i/T_e)$  with  $L_n$  being the density gradient scale length, which is satisfied for all the data set in this series of experiments. The operation with a fixed magnetic geometry enables  $s/q$  to remain nearly constant. One possible concern is that  $T_i/T_e$  may cause a difference in the ion heat transport. However, as shown in Fig. 6,  $T_i/T_e$  remained at a nearly constant value of 1.1–1.3 at  $r/a = 0.6$  for both the hydrogen and deuterium plasmas as  $Q_i$  was varied. Accordingly, there is no expected difference in the linear ITG threshold between hydrogen and deuterium. The average threshold value is indicated as a broken line in Fig. 5. All the experimental data are above the threshold value for the ITG unstable region at  $L_{T_i} < L_{T_i}^c$ . While the  $L_{T_i}$  values in the sufficiently heated phase are clearly smaller for deuterium than those for hydrogen, it is hard to identify whether the ITG threshold  $L_{T_i}^c$  becomes certainly smaller for deuterium in this series of experiments.

In summary, the dependence of the ITG scale length on the hydrogen isotope mass was examined in conventional  $H$ -mode plasmas. Identical spatial profiles for the density and temperature that led to the same  $W_{th}$  were obtained for hydrogen and deuterium plasmas. The ion conductive heat flux  $Q_i$  for hydrogen became approximately two times that for deuterium, corresponding to a required heating power to sustain the same  $W_{th}$  value that was two times as large for hydrogen. Hence, the  $\chi_i$  values for hydrogen were higher, explicitly throughout the minor radius, than those for deuterium at the same  $L_{T_i}$ . On the other hand, the

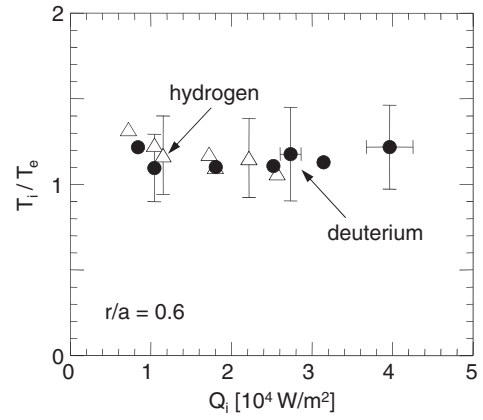


FIG. 6.  $T_i/T_e$  values as a function of  $Q_i$  at  $r/a = 0.6$ .

$\nabla T_i/T_i$ , or the inverse of  $L_{T_i}$ , required for a given  $\chi_i$  increased by a factor of  $\sim 1.2$  for deuterium compared with that for hydrogen. These results show that, for a given ion heat diffusivity,  $L_{T_i}$  is reduced by increasing the hydrogen isotope mass in  $H$ -mode plasmas.

The results also offer the key to understanding the mechanism of a better confinement for a heavier isotope based on the physics picture involving the large-scale interaction of the edge pedestal and core components. The smaller  $L_{T_i}$  helps primarily the core plasma energy to increase with a heavier isotope species. However, as presently understood,  $H$ -mode confinement is not determined individually by the core and pedestal components, but by the relationship of two physics processes: (1) the increase of the pedestal temperature as a boundary condition affecting the reduction in the core heat transport through the profile stiffness, and (2) the increase in the total poloidal beta  $\beta_p$  or the Shafranov shift improving the edge stability limit [19–22]. Thus, the enhanced core confinement for a heavier isotope species caused by a smaller  $L_{T_i}$  might also help lead to an improvement in the edge stability due to the increased  $\beta_p$ . An investigation of the overall  $H$ -mode confinement for hydrogen and deuterium plasmas as determined by the processes described above will be the subject of a future study.

The authors are grateful to Dr. M. Mori, Dr. T. Ozeki, Dr. T. Fujita, Dr. S. Ide, Dr. T. Suzuki, and Dr. M. Honda for their encouragement and helpful advice. The diligent support of the JT-60 Team is also cordially acknowledged.

- [1] D. P. Schissel *et al.*, *Nucl. Fusion* **29**, 185 (1989).
- [2] M. Bessenrodt-Weberpals *et al.*, *Nucl. Fusion* **33**, 1205 (1993).
- [3] S. A. Sabbagh *et al.*, in *Plasma Physics and Nuclear Fusion Research 1994*, Proceedings of the Fifteenth International Conference on Plasma, Seville, 1994, Vol. 3 (IAEA, Vienna, 1994), p. 663.
- [4] J. G. Cordey *et al.*, *Nucl. Fusion* **39**, 301 (1999).

- [5] M. Kotschenreuter, W. Dorland, M. A. Beer, and G. W. Hammett, *Phys. Plasmas* **2**, 2381 (1995).
- [6] A. Dimits *et al.*, *Phys. Plasmas* **7**, 969 (2000).
- [7] H. Urano, Y. Kamada, H. Shirai, T. Takizuka, S. Ide, T. Fujita, and T. Fukuda, *Nucl. Fusion* **42**, 76 (2002).
- [8] G. Tardini *et al.*, *Nucl. Fusion* **42**, 258 (2002).
- [9] A. G. Peeters *et al.*, *Nucl. Fusion* **42**, 1376 (2002).
- [10] D. R. Mikkelsen *et al.*, *Nucl. Fusion* **43**, 30 (2003).
- [11] H. Urano, T. Takizuka, Y. Kamada, N. Oyama, H. Takenaga, and the JT-60Team, *Nucl. Fusion* **48**, 045008 (2008).
- [12] ITER Physics Basis, *Nucl. Fusion* **39**, 2175 (1999).
- [13] H. Shirai, T. Takizuka, Y. Koide, O. Naito, M. Sato, Y. Kamada, and T. Fukuda, *Plasma Phys. Controlled Fusion* **42**, 1193 (2000).
- [14] H. Urano, N. Oyama, K. Kamiya, Y. Koide, H. Takenaga, T. Takizuka, M. Yoshida, Y. Kamada, and the JT-60Team, *Nucl. Fusion* **47**, 706 (2007).
- [15] N. Aiba, M. Furukawa, M. Hirota, N. Oyama, A. Kojima, S. Tokuda, and M. Yagi, *Nucl. Fusion* **51**, 073012 (2011).
- [16] P. Mantica *et al.*, *Phys. Rev. Lett.* **107**, 135004 (2011).
- [17] H. Urano, H. Takenaga, T. Fujita, Y. Kamada, Y. Koide, N. Oyama, M. Yoshida, and the JT-60Team, *Nucl. Fusion* **48**, 085007 (2008).
- [18] S. C. Guo and F. Romanelli, *Phys. Fluids B* **5**, 520 (1993).
- [19] Y. Kamada, N. Oyama, S. Ide, Y. Sakamoto, A. Isayama, T. Fujita, H. Urano, T. Suzuki, and M. Yoshida, *Plasma Phys. Controlled Fusion* **48**, A419 (2006).
- [20] C. F. Maggi *et al.*, *Nucl. Fusion* **47**, 535 (2007).
- [21] P. B. Snyder *et al.*, *Nucl. Fusion* **47**, 961 (2007).
- [22] A. W. Leonard, R. J. Groebner, T. H. Osborne, and P. B. Snyder, *Phys. Plasmas* **15**, 056114 (2008).